Deconvolution of the first "illite" basal reflection

Deconvolution of the first "illite" basal reflection

by *W.B. Stern, J. Mullis, M. Rahn* and *M. Frey*[1]

Abstract

Aside from a change in the half-width of the illite basal reflection with metamorphic grade, there is often a marked asymmetry, or tailing, which is not present in well-crystallized sheet silicates like muscovite or chlorite. This asymmetry is explained by the presence of an additional phase, with a slightly different d-spacing than the illite first basal reflection, and a much larger half-width. In some cases the apex (peak maximum) of the illite first basal reflection and mentioned second phase is clearly resolved, in other cases, however, only a certain tailing is visible, or a change in line shape of "illite", when the apexes of both reflections have the same d-spacing.

If two phases contribute to a reflection, the evaluation of one single half-width tends to be misleading. The present study tries to deconvolute the two reflections – one belonging to illite-muscovite, the other presumably to a smectitic phase – by means of a mathematical profile fit procedure.

Measurements and evaluations carried out on four decalcinated < 2 μm fractions (air-dried, glycolated, heated smear slides) extracted from limestone/slates of different metamorphic grade reveal that the half-width of the illite varies slightly (from 0.37 to 0.20 δ° 2Θ) with rising metamorphic grade, whereas the half-width of the smectitic phase evolves strongly (from 1.47 to 0.47 δ° 2Θ), the average chemical composition of these fractions remaining virtually constant, when volatiles are disregarded.

Keywords: X-ray diffraction, illite-crystallinity, half-width, peak-profile, deconvolution, chemical composition, diagenesis/metamorphism.

Introduction

The relation between particle size of a powdered specimen, and the shape of diffracted X-rays was first described by SCHERRER as early as 1918. Application to clay mineralogy goes back to the early sixties, when WEAVER (1960) used peak heigths of the first basal spacing of illite to derive a "Sharpness ratio" as an indicator of crystallinity.

Later (KÜBLER, 1964), the peak width at half peak maximum came into use, first expressed as distance in mm, and later (KISCH, 1983) as angular width δ° 2Θ. This half-width has become a widely accepted criterion in the study of diagenetic or very low-grade metamorphic rocks, i.e. when the degree of ordering must be evaluated (KÜBLER, 1990). Recently (LANSON and CHAMPION, 1991), a decomposition of "the near-10 Å band" was proposed using 2 to 4 Gaussian functions attributed to illite, detrital muscovite, smectite, and mixed layer illite/smectite.

The aim of this methodological study is to prove, that

– the first basal reflection of "illite"[2] (treated as a single peak when used as an indicator of diagenetic and low-grade metamorphic grade), actually consists of at least two distinct reflections, namely illite-muscovite and a smectitic phase;
– the X-ray patterns of these superimposed reflections can be deconvoluted mathematically, and the respective half-widths and peak positions determined;
– the calculated half-widths and peak positions bear additional and relevant information to be

[2] Quotation marks ("..") in connection with illite are used in this text, when the unresolved basal reflection at 10 Å of illite and a smectite phase is referred to. "Smectitic phase" is used as a general term for smectite/illite interlayers; smectite s.s. (displaying a 17 Å reflection after glycolation) is not present in the sampels studied here.

[1]Institute of Mineralogy and Petrography, Basel University, Bernoullistrasse 30, CH-4056 Basel, Switzerland.

used in studies on low-grade clay mineral bearing rocks;

– the presence and crystallinity of illite and the smectitic phase are not only correlated with metamorphic grade, but possibly also with bulk chemical composition of the < 2 μm fraction and the release of hydrocarbons and water.

The present study does not try to unravel the controversial aspects of clay mineralogy nomenclature.

Specimens and their provenance

Three localities from a profile of the Reuss valley were sampled; all three localities are in the external part of the Central Alps (FREY et al., 1980, BREITSCHMID, 1982, MULLIS et al., in prep.). The collected specimens represent lithologically different rocks, formed under diagenetic, low-grade and high-grade anchizonal conditions. For further details see table 1.

Tab. 1   Provenance of samples

Specimen	Locality	Coordinates	Tectonic / stratigraphic position	Lithology	Maximum mineral assemblage	Fluid composition (mole-%)	T (°C) P (MPa)	Vitrinite reflectance (%)	Literature
Mu-27	Zingel	699.850 / 209.200	Border Chain Drusberg-schichten	marly limestone	qz cc chl ill ill-sm ab dol org.mat.	H2O 11.9 H2 1.4 N2 2.2 CO2 0.8 CH4 76.7 HHC 7.1	120-150°C <120 MPa	Rm = 1.7	BREITSCHMID, 1982 MULLIS, 1988
Mu-35	Attinghausen	689.300 / 192.220	N Helvetic Flysch Dachschiefer	calcareous slate	qz cc ill ill-sm chl dol ab org.mat.	H2O 97.7 CH4 1.3 NaCl 1.0 H2O 5.7* CH4 91.0 CO2 2.6 NaCl 0.0	262-+4°C 180 MPa	Rm = 3.75 3.9 Rmax= 4.5 4.7	FREY et al., 1980a BREITSCHMID, 1982 MULLIS et al., in preparation
Mu-685a	Scheidnössli	692.300 / 187.750	Autochthonous cover "Trias"	siliceous dolomitic slate	qz ill dol chl cc ab ill-sm	H2O 96.9 CH4+ CO2 0.8 NaCl 2.3	>270°C >180 MPa	Rm = 5.1+	BREITSCHMID, 1982
Mu-685b	Scheidnössli	692.360 / 187.820	Autochthonous cover "Aalenian"	slate	qz ill chl pyroph cc dol ab org.mat		>270°C >180 MPa	Rm = 5.1+	BREITSCHMID, 1982

+ sampled on the western side of the Reuss valley   * methane-rich inclusions

Tab. 2   XRD-data

Specimen	Seq	Off-line HW-graph	Off-Line H-hight	HW°2θ	Split-Pearson d(Å)	HW°2θ	Area	Hight	Rel-%	Pearson Deconvolution Smectitic phase d(Å)	HW°2θ	Area	Hight	Illite d(Å)	HW°2θ	Area	Hight	Rel%
Mu-27	1	1.40	2834	1.33	9.93	1.52	842	475	17.0	10.71	1.47	644	395	9.93	0.33	117	295	10.1
Mu-27	2	0.61	2786	0.55	9.93	0.51	330	489		11.39	1.99	210	96	9.94	0.46	291	471	7.8
Mu-27	3		3418	0.59	9.97	0.74	529	564	14.0	11.40	1.69	280	130	9.93	0.27	152	295	6.9
Mu-27	4		3072	1.12	9.93	1.10	683	522	14.6	10.71	1.38	546	354	9.98	0.42	192	383	6.4
Mu-27	5		4219	0.76	10.00	0.79	812	812	7.4	10.45	1.07	553	445	9.98	0.41	252	558	5.5
Mu-27	6		4959	0.63	9.98	0.68	809	929	8.1	10.39	0.93	672	510	9.98	0.36	269	671	4.7
Mu-35	1	0.58	2530	0.55	9.93	0.62	351	425	12.2	10.39	1.12	421	271	9.93	0.29	117	342	6.7
Mu-35	2	0.47	2565	0.42	9.94	0.47	495	509	6.0	10.10	1.07	290	201	9.93	0.30	146	339	5.0
Mu-35	3		2843	0.44	9.95	0.47	551	572	5.7	10.10	0.96	482	332	9.93	0.24	100	322	5.4
Mu-35	4		2585	0.61	9.93	0.68	467	481	9.4	10.33	0.91	379	302	9.93	0.32	122	348	5.6
Mu-35	5		3330	0.51	9.95	0.54	441	633	7.0	10.21	0.68	400	403	9.93	0.26	121	425	5.0
Mu-35	6		3630	0.46	9.87	0.47	584	751	4.2	10.21	0.70	348	326	9.87	0.30	192	565	3.7
Mu-685a	1	0.35	8320	0.35	9.93	0.34	797	1650	3.0	10.16	0.47	511	736	9.93	0.23	319	1266	2.9
Mu-685a	2	0.31	10024	0.30	9.92	0.31	906	2025	2.3	10.16	0.57	387	477	9.93	0.25	522	1726	1.9
Mu-685a	3		9671	0.33	9.96	0.33	940	1963	3.1	10.10	0.42	775	1149	9.93	0.20	260	1209	4.1
Mu-685a	4		9636	0.31	9.90	0.31	842	1940	3.5	10.04	0.38	655	1149	9.87	0.18	243	1226	4.7
Mu-685a	5		11615	0.28	9.92	0.29	951	2303	2.6	10.10	0.54	418	654	9.93	0.22	452	1784	3.8
Mu-685a	6		11505	0.26	9.94	0.29	940	2331	2.6	10.10	0.39	589	1070	9.93	0.19	354	1667	3.1
Mu-685b	1	0.46	6965	0.38	10.01	0.40	649	1238	7.3	10.16	0.62	663	721	9.98	0.21	232	845	3.2
Mu-685b	2	0.46	4972	0.39	9.98	0.40	661	994	6.0	10.00	0.63	574	653	9.95	0.19	83	397	2.9
Mu-685b	3		6802	0.37	9.97	0.38	821	1322	4.1	10.02	0.64	745	857	9.97	0.18	112	548	2.8
Mu-685b	4		6788	0.36	9.93	0.37	666	1288	4.9	10.04	0.66	487	589	9.93	0.23	230	834	4.4
Mu-685b	5		7838	0.33	9.94	0.35	720	1462	4.8	10.04	0.55	573	714	9.93	0.21	277	956	3.1
Mu-685b	6		7780	0.34	9.97	0.34	783	1552	3.3	10.04	0.45	944	1198	9.93	0.17	121	644	4.5

Seq-1   air dried smear slide   Seq-4   tempered 2h at 150°C   Rel.-%   Reliability Percentage :
Seq-2   glycolated   Seq-5   tempered 16h at 250°C   accordance of fitted
Seq-3   air dried 20h 20°C   Seq-6   tempered 3h at 350°C   vs measured diffractogram

Methods of investigation

Sample preparation: From the hand specimens about 60 to 80 g were taken. Each sample was then cut into small pieces, which were then ground with a tungsten carbide disk mill avoiding grinding times longer than 30 seconds. In order to remove carbonates, the samples were treated with 2 n HCl and washed with distilled water before separating the fraction of < 2 μm using Atterberg cylinders. Separated fractions were taken to produce measuring samples on glass slides by sedimentation of the fraction as aqueous suspension on the slide. The average mass per unit area was determined to be around 5 mg/cm². The samples Mu-27 and Mu-35a have been treated with a saturated $CaCl_2$-solution for 12 hours before preparing slides. All samples were prepared under air-dried, and glycolated conditions; glycolated smear slides were dried after measurement, and heated at intervals of 150°, 250°, 350° (see Tab. 2).

XRD measurements: Smear slides were measured by using both, a conventional diffractometer without computational on-line facilities and with a modern instrument; for technical details see table 3a. Evaluation was done off-line graphically on chart-strip diffractograms, or with a computer on background-subtracted reflections.

XFA: A 150 mg subsample of the < 2 μm fraction was taken for a quantitative analysis of chemical main constituents. For technical details see table 3b.

H_2O, C, CO_2: Combustion analysis was done on subsamples (50 mg each). For technical details see table 3c.

Tab. 3 Instrumentation and technical details

A. X-ray diffraction

	Philips PW-1360	Siemens D-500
Tube	Cu 40 kV 25 mA	Cu 40 kV 30 mA
Filter	Ni	none
Monochromator	none	Graphite, secon.
Slits	1° 0.2 mm 1°	3°/3°-3°/1°-.005° 2Θ automat. divergence, slit; increment = 0.05° 2Θ
Goniometer	2 and 0.5° 2Θ pmin	0.3° 2Θ per minute
Counter	sealed	sealed
Computer	none	Sicomp 32-20
Software	none	Diffrac-AT
Evaluation	off-line, graph.	Background subtraction, fit, Pearson deconvolution

B. X-ray fluorescence analysis

	Spectrace-5000	Siemens SRS-303
Tube	W thin side window	Rh and window
Excitation	simultaneous	sequential
Specimen	30 mg on foil 40 mm O	32 mm glass beads (XV)
Software	EDXRF, Fundparam	Spectra-AT
Evalution	Routine GL-III	Routine QUANTXV
Elements	18 analyzed	32 analyzed

C. Determination of volatile components

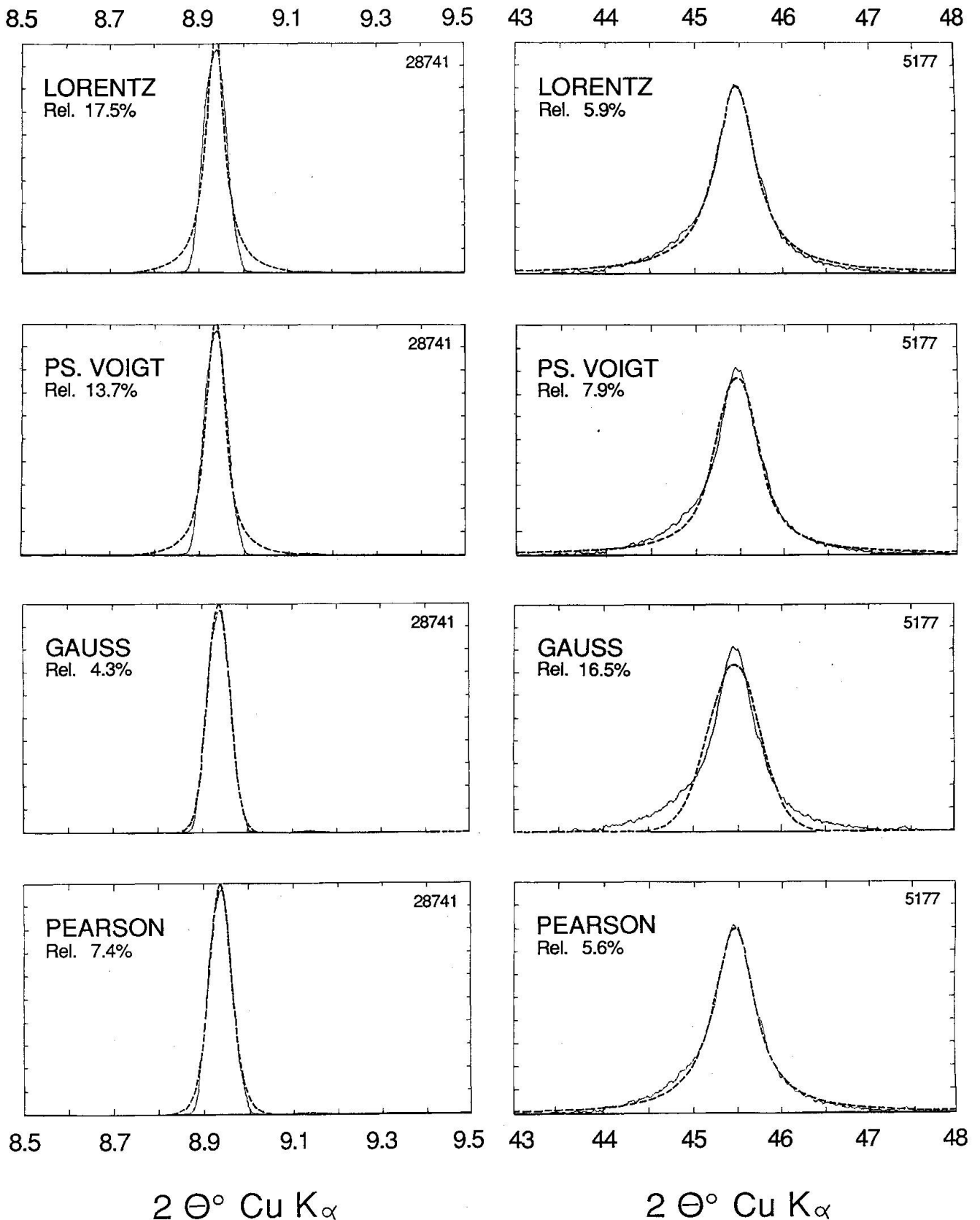|	LECO RC-412, quartz oven temp. controlled
Temp. range	dynamic, 100 to 1100 °C, ramping 70 °C p. min.
Specimen	50 mg < 2 μm fraction
Evaluation	graphically

Fig. 1   X-ray diffractograms of a well crystallized sheet silicate (2 M1 muscovite single crystal from Venkateshwara pegmatite, India, HW-0.06° 2Θ, left side), and of a weak basal reflection (smear slide B99MO, HW = 0.55° 2Θ, right side). No explicit tailings visible. After background subtraction both reflections were fitted by using various mathematical functions (broken lines: Lorentz, Pseudovoigt, Gauss, Pearson). According to peak height either Gauss, Pearson (Fig. 1, left side), or Pearson, Lorentz (Fig. 1, right side) functions fit best; when peak height is variable, preferably a Pearson function should be used. Each graph bears its reliability percentage and full scale intensity.

Results and discussion

A remarkable feature of the first basal reflection of "illite" is the often prominent asymmetry or tailing. Other minerals, like muscovite, kaolinite or chlorite display reflections at similar diffraction angles but do not show this phenomenon (Fig. 1, left side). This tailing might be explained by the presence of a second, more or less hidden reflection from one or several additional phases, such as a smectitic mineral ore illite-smectite interlayers or by the presence of open layers on the edges of illite, or an amorphous component.

If several reflections are hidden within the so-called "illite" peak, any half-width determination based on one single reflection is misleading. When two quasi-symmetrical peaks of different half-width and similar d-value are super-imposed, a signal results which can only be evaluated by appropriate fitting procedures and deconvolution programs (such programs have been available commercially for many years, and applied for poorly crystallized minerals by HANDSCHIN, 1990; KÜBLER et al., 1990). Provided that counting statistics are adequate and that the background is suitably modelled and subtracted, reflections are undisturbed at their foot; they can be deconvoluted with iteratively varying d-values and half-widths (Fig. 2). Since a correct deconvolution ends up with – at least – two different d-values, half-widths, and peak areas, new arguments come into consideration; broad peaks from diagenetic environments, and disregarded so far (e.g. PETSCHIK, 1989), can be differentiated this way.

Various mathematical functions are, in principle, able to fit a symmetrical diffraction curve (Fig. 1). A large, symmetrical peak is best matched by a Gauss or a Pearson function, whereas a weak peak is best matched by a Pearson or a Lorentz function. From empirical considerations, Pearson functions are recommended when peaks of various hights have to be fitted. Fitting and deconvolution have their limitations when counting statistics are poor.
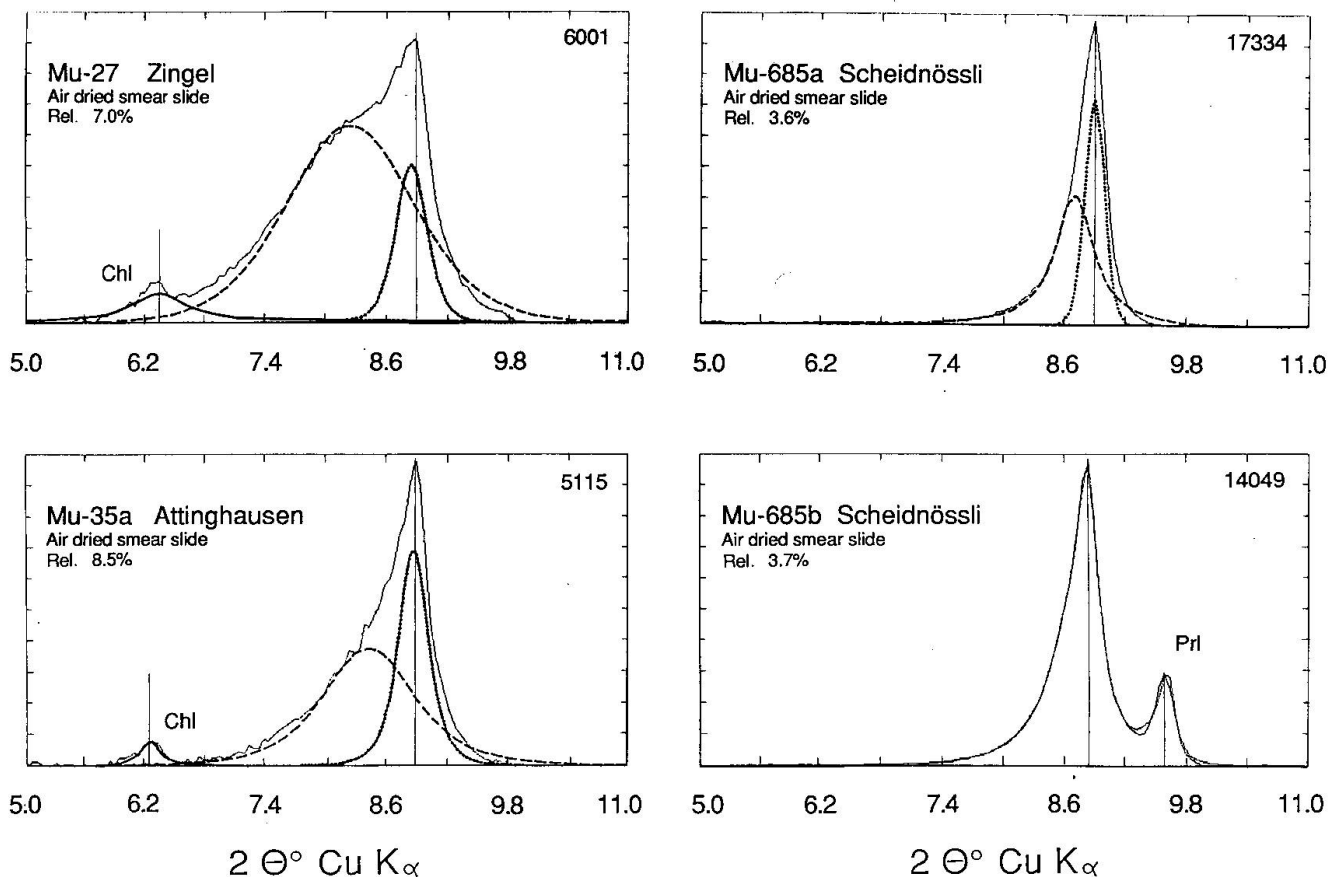
Fig. 2 XRD diffractograms of four samples from the Reuss valley profile (diagenetic to high-grade anchizone): air-dried < 2 μm fractions after background subtraction. The Pearson functions of illite and the smectitic phase, obtained after deconvolution are shown as dashed/broken lines. Diagenetic limestone MU-27 displays a beginning distinction of a second hump-like reflection at 10.7 Å, attributed to a smectitic phase. Chlorite = Chl, Pyrophyllite = Pre.
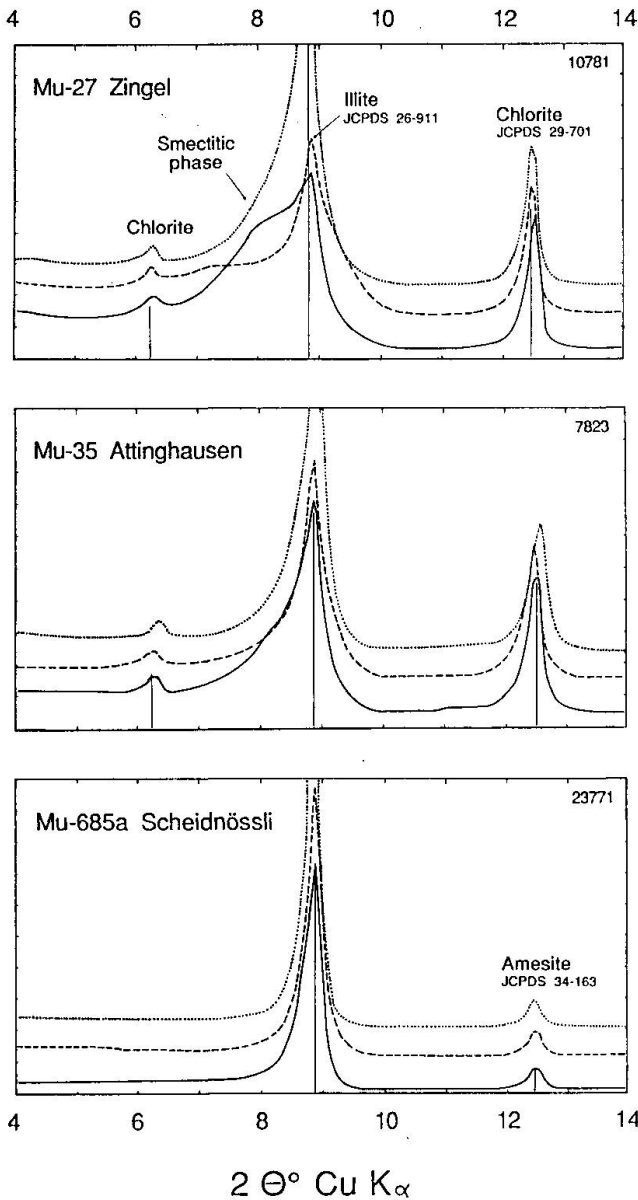
Fig. 3a) Un-deconvoluted diffractograms of air-dried (line), glycolated (broken line) and tempered (350 °C, dashed) smear slides. Full scale intensity indicated on the upper right.

Fig. 3b) Half-width ($\delta°$ 2Θ at half maximum, obtained by deconvolution) of illite and the smectitic phase. Numbers on the x-axis refer to specimen treatment (Tab. 2):

1 air-dried smear slide   2 glycolated smear slide
3 air-dried after glycolation   4 tempered at 150 °C
5 tempered at 250 °C   6 tempered at 350 °C

Half width ($\delta°$ 2Θ) after deconvolution:

| | Illite HW | | | Smectitic phase | |
	aver.	std. dev.	d ($\overset{\circ}{A}$)	HW	d ($\overset{\circ}{A}$)
Mu-27	0.37	0.063	9.96	1.47	10.71
Mu-35	0.29	0.026	9.92	1.12	10.39
Mu-685a	0.21	0.023	9.92	0.47	10.16
Mu-685b	0.20	0.019	9.95	0.62	10.16

In the case of illite, averages and standard deviations were calculated of data obtained on air-dried and heated smear slides. For the smectitic phase, no statistical data were extracted since heating alters the structure of this phase rapidly (Fig. 3b).

The effect of glycolation and heating on illite and smectitic phase can be seen on figure 3b. Glycolation has no impact on illite half-width, but a strong influence on the smectitic phase from diagenetic rock Mu-27; 20 hours of air-drying do not reduce the half-width to the original value (comparing sequence 1 and 3). Because the "illite" half-width of glycolated smear slides does not differ from the air dried ones, one migth conclude that glycolation is not necessary when peak deconvolution is performed to determine an illite half-width. For differentiation, of the smectitic phase, however, glycolation remains an essential diagnostic tool in order to distinguish between smectite and mixed-layer smectite (both labelled here "smectitic phase").

There is a correlation between the respective half-widths of illite and the smectitic phase deter-

In this case, the specimen has to be measured again with a lower scanning speed. It would easily be possible to improve the apparent fitting quality by incorporating reflections of additional phases in the deconvolution procedure (Lanson, CHAMPION, 1991). This approach, however, is correct only, when there is clear mineralogical or petrographical evidence for further phases present.

Measurements on air-dried, glycolated and heated smear slides of the four mentioned localities ranging from the diagenetic zone in the north (Zingel) to the high-grade anchizone in the south (Scheidnössli) display changing half-widths for illite, and smetitic phase as well (Fig. 3a).
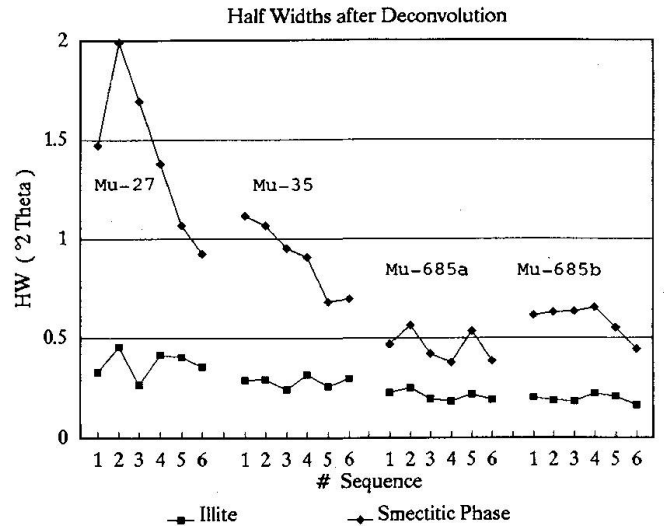
Half Widths of Illite and Smectitic Phase after Deconvolution
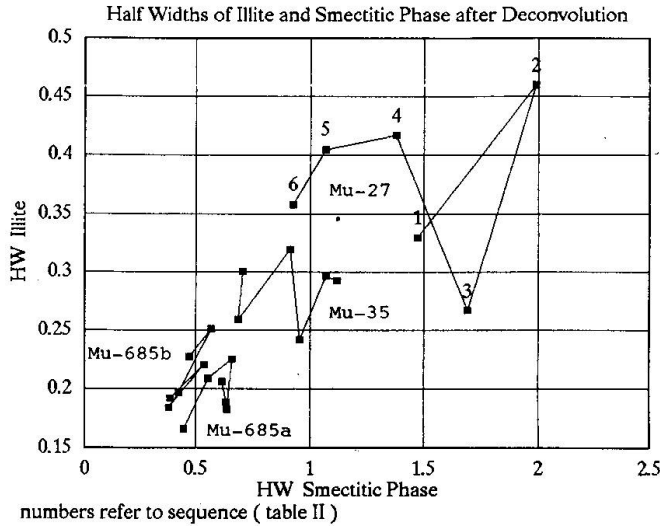
numbers refer to sequence (table II)

Fig. 4a Half-widths, obtained by deconvolution: smectitic phase vs illite, tie-lines between data obtained on the same sample; for explanation of the numbers refer to figure 3. The half-width of both phases is positively correlated, variation of data decreasing from diagenetic (Mu-27) to low-grade (Mu-35) and high-grade anchizonal conditions (Mu-685a, b).

mined by peak deconvolution (Fig. 4a). Since the numerical variation of the latter is larger, the smectitic phase might be more suitable for crystallinity measurements than illite. Deconvolution reveals not only data on half-widths, but on respective d-values as well (Fig. 4b). The peak position of the smectitic phase changes strongly parallel to the half-width, whereas for illites the half-width only is changing.
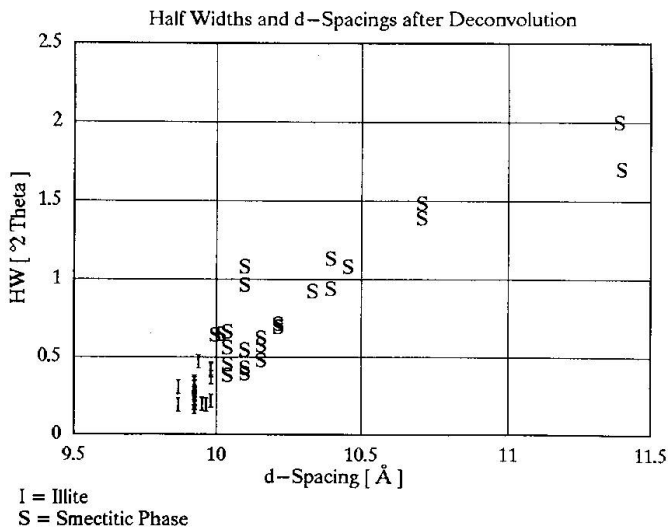

Half Widths and d—Spacings after Deconvolution

I = Illite
S = Smectitic Phase

Fig. 4b Half-width and peak position of smectitic phase (S) and illite (I) after deconvolution). HW and d-value of smectitic phases change from rocks formed under diagenetic (Mu-27) to high-grade anchizonal conditions (Mu-685), whereas illite changes only its half-width to a limited extend.
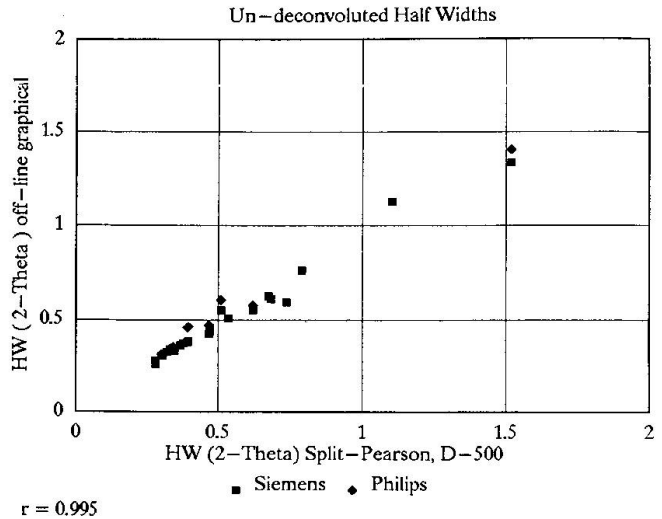

Un—deconvoluted Half Widths

■ Siemens ◆ Philips

r = 0.995

Fig. 5 Complex signals treated as one single reflection either graphically off-line (traditionally called "Illite Crystallinity"), or by asymmetrical curve fitting (Split-Pearson function). The data correspond well (r = 0.995 for N = 14), even when results from different diffractometers are compared. On the x-axis HW data obtained by Split-Pearson fitting are recorded, on y-axis the graphically determined HW of Philips and Siemens runs respectively.

From the correlation of illite and smectitic half-widths it might be expected that the previous crystallinity measurements done on the "illite" peak would serve as well as any sophisticated peak deconvolution. In fact, with advanced XRD technology, an asymmetrical reflection can be treated as a single peak and the half-width determined by a split-Pearson function (among others). Half-widths obtained this way correspond fairly well with graphically determined data (Fig. 5). This procedure, however, reaches limits when the smectitic part begins to appear as an individual reflection, as is the case with Mu-27 (see Figs 2, 3a). Since much information is lost when "illite" is treated as a single peak, deconvolution is strongly recommended.

The volatile content of the < 2 µm fractions, determined over a temperature range from 100 to 1100 °C displays a complex pattern (Fig. 6 a, b). Though dried for several hours at 105 °C, a considerable proportion (between 5 and 20% of water) is still present. It is largely released by 200 °C. Further release of H_2O takes place around 300 and 450 °C and is accompanied by a slight loss of carbon; most probably hydrocarbons are cracked and/or burnt. The major part of carbon (80% of the total, Fig. 6a), however, is released between 500 °C (in diagenetic rock Mu-27) and nearly 600° (in high-grade anchizonal rock Mu-685a).

The main release of water (50 to 70% of the total, Fig. 6b) occurs between 600 and 720 °C, again
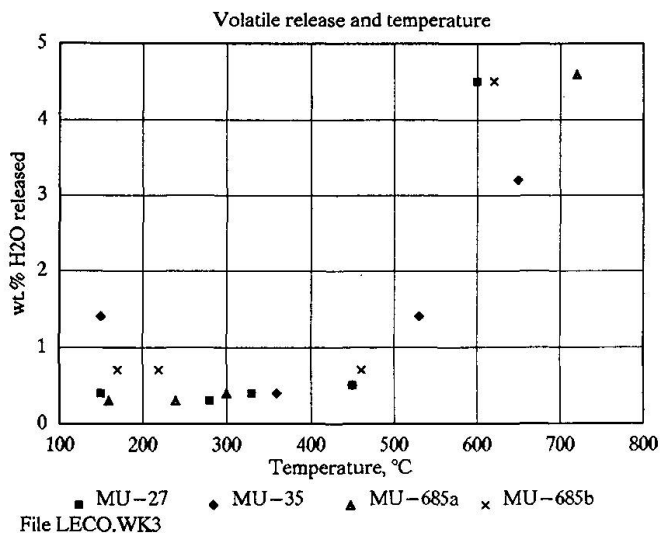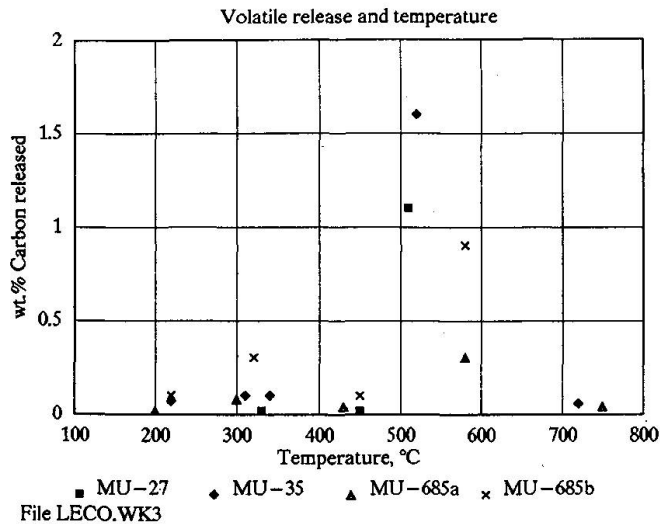
Volatile release and temperature

■ MU–27   ◆ MU–35   ▲ MU–685a   ✕ MU–685b
File LECO.WK3

Volatile release and temperature

■ MU–27   ◆ MU–35   ▲ MU–685a   ✕ MU–685b
File LECO.WK3

Fig. 6   Volatile contents (carbon, Fig. 6a and water, Fig. 6b) of < 2 µm fractions. The main fractions of carbon and water are released at lower temperatures in case of diagenetic (Mu-27) than in high-grade anchimetamorphic samples (Mu-685).

starting at lower temperatures in diagenetic rocks, and at higher temperatures in the anchizonal rocks. This release is most probably linked with decomposition of clay minerals.

The bulk chemical composition of the four < 2 µm fractions is very similar, except for alumina in sample Mu-685b, where XRD reveals the presence of pyrophyllite (Tab. 4, Fig. 2). < 2 µm fractions plot in the same field as certain illites taken from literature (microprobe data from CHAMLEY et al., 1990, Fig. 7). Although it is not clear whether microprobe analyses of clay minerals are at all feasible – the analytical resolution being an order of magnitude off the grain size of clay minerals – microprobe data may nevertheless give information on chemical trends: illite plots between muscovite

s.s. and chlorite, smectite bridging the gap between illite and chlorite. Because all < 2 µm fractions contain chlorite (either clinochlore – or septechlorite – like type) in minor proportions, it might be expected that their presence is balanced by the occurrence of muscovitic illite. The existence of a poorly crystallized phase demonstrated by diffractometry and displaying a large half-width, a d-spacing close to illite (002), and a marked sensitivity to glycole, is then chemically interpreted as a transition between chlorite-smectite on one hand, and illite-muscovite on the other. Hence this phase is called here "smectitic" phase.

Tab. 4   Chemical analysis (WD-XFA) of the < 2 fraction

wt%	Mu-27	MU-35	Mu-685a	Mu-685b
SiO_2	52.88	52.29	49.93	50.78
Al_2O_3	24.35	22.67	25.19	28.58
Fe_2O_3t	2.10	4.52	4.34	3.99
MnO	0.00	0.00	0.00	0.00
MgO	3.44	3.09	2.89	0.86
CaO	0.30	0.23	0.35	0.21
Na_2O	0.94	0.76	0.59	0.44
K_2O	5.38	6.40	7.90	5.67
TiO_2	0.64	0.84	0.90	1.13
P_2O_5	0.72	0.87	1.30	0.54
LoI	9.08	8.32	6.48	7.51

Conclusions

1. The first basal reflection of "illite" which has been treated so far as a single peak (when "Illite-Crystallinity" was derived based on width measurements at half peak maximum) consists of at least two distinct reflections which can be assigned individual half-widths on d-spacings. These reflections can best be resolved by a mathematical fit procedure on the basis of Pearson functions.

2. The reflection corresponding to a d-spacing of 9.9 Å is attributed to an illite-muscovite phase which is unaffected by glycolation and mild tempering. The half-width of this reflection changes slightly with increasing diagenesis and metamorphic grade, but keeps the d-spacing nearly constant.

3. The broad reflection displaying d-spacings between 10 and 10.7 Å is attributed to a smectitic phase. It is affected by glycolation and mild tempering. Half-width and d-value change strongly with increasing diagenesis and metamorphic conditions.

4. Since a mathematical deconvolution of superimposed X-ray reflections is easily possible provided that counting statistics are adequate, the half-

Al₂O₃

Legend:

C   chlorites (Chamley)

I   illites (Chamley)

S   smectites (Chamley)

J   illites (DHZ)

M   white micas (DHZ)

P   pyrophyllites (DHZ)

●   Mu 27, 35,
     685a, 685b } (<2µ)

Fe₂O₃, MgO   Na₂O, K₂O, CaO

Fig. 7 Chemical data of > 2 µm fractions and of minerals (CHAMLEY et al., 1990 microprobe analyses, DHZ = DEER et al., 1962) plotted in a triangular diagram of the chemical main constituents. The bulk chemistry of the < 2 µm fractions (Tab. 4) occupies a narrow compositional field very close to certain illites, and laying between muscovite and chlorite/smectite.

width of an illitic phase can be determined without glycolation, even in diagenetic rocks.

5. When the first basal reflection of "illite" is evaluated as a single, asymmetrical peak by using Split-Pearson functions, the half-widths obtained correspond fairly well with graphically determined half-widths, obtained from an older diffractometer.

6. Shape and half-width of the first basal reflection of "illite" are primarily influenced by the metamorphic grade of the host rock. They are defined by the half-widths of illite and the smectitic phase, by their peak positions and the respective peak areas (the latter in principle being linked with their mass proportions). The amount of illite and the smectitic phase present could, theoretically, depend on the bulk chemical composition.

7. The half-width determination of the unresolved "illite" first basal reflection, as it has been

used so far, becomes invalid when a second, hump-like reflection begins to appear at the long-wavelength side of illite (e.g. the case specimen Mu-27). Deconvolution permits the quantification of changes in half-width and d-spacing of smectitic and illitic fractions respectively, both of which are correlated with vitrinite reflectance (FREY et al., 1980; BREITSCHMID, 1982) and also with the devolatilization of carbon- and hydrogen-bearing chemical phases.

References

BREITSCHMID, A. (1982): Diagenese und schwache Metamorphose in den sedimentären Abfolgen der Zentralschweizer Alpen (Vierwaldstättersee, Urirotstock). Eclogae geol. Helv. 75/2, 331–380.

CHAMLEY, DEBRABANT, P., ROBERT, C., MASCLE, G., REHAULT, J.-P. and APRAHAMIAN, J. (1990): Mineralogical and geochemical investigations of latest Miocene deposits in the Tyrrhenian Sea (ODP leg 107). In: KASTENS, K., MASCLE, J. et al. (Ed.): Proc. Ocean Drill. Progr, Sci. Res, Vol. 107B, 153–167.

DEER, W.A., HOWIE, R.A. and ZUSSMAN, J. (1962): Rock Forming Minerals, Vol. 3: Sheet Silicates, Longmans, London, 270 p.

FREY, M., TEICHMÜLLER, M., TEICHMÜLLER, R., MULLIS, J., KÜNZI, B., BREITSCHMID, A., GRUNER, U. and SCHWIZER, B. (1980): Very low grade metamorphism in external parts of the Central Alps: Illite crystallinity, coal rank and fluid inclusion data. Eclogae geol. Helv. 73, 173–203.

HANDSCHIN, R. and STERN, W.B. (1989) : Preparation and Analysis of Microsamples for X-ray Diffraction and -Fluorescence. Analyt. Appl. Note 319. Siemens Order Nr. A19100-E689-B14-Vl-7600.

HANDSCHIN, R. (1990): Méthode pratique d'analyse de micro-échantillons pour diffraction et flourescence X. Quelques exemples. Annual meeting Swiss Soc. Mineral. Petrogr., Poster Session, Geneva.

KISCH, H. (1983): Mineralogy and petrology of burial diagenesis (burial metamorphism) and incipient metamorphism in clastic rocks. In: LARSEN, E. and CHILINGAR, G.V. (Ed.): Diagenesis in Sediments and Sedimentary Rocks, 2. ed., 289–493 and 513–541. Elsevier, Amsterdam.

KÜBLER, B. (1964): Les argiles, indicateurs de métamorphisme. Rev. Inst. Franç. Pétrol. Vol. XIX, 1093–1112.

KÜBLER, B. (1968): Evaluation quantitative du métamorphisme par la cristallinité de l'illite. Bull. Centre Rech. de Pau – SNAP, 2, 385–397.

KÜBLER, B. (1990): Cristallinité de l'illite et mixed-layers: brève révision. Schweiz. Mineral. Petrogr. Mitt. 70, 89–93.

KÜBLER, B., JANTSCHIK, R. and HUON, S. (1990): Minéralogie et granulométrie des poussières éoliennes dites "Sahariennes", du 24 avril 1989 a Neuchâtel. Leur importance pour l'environnement, les sols et les sédiments. Bull. Soc. neuch. Sc. Nat. 113, 75–98.

LANSON, B. and CHAMPION, D. (1991): The I/S-to-illite reaction in the late stage diagenesis. Amer. Jour. Sci., 291, 473–506.

MULLIS, J., DUBESSY, J., POTY, B. and O'NEIL, J. (in prep.): Fluid regime during the late stages of continental collision: a case study based on fluid inclusion data from fissure quartz along the Basel–Chiasso Geotraverse.

PETSCHICK, R. (1989): Zur Wärmegeschichte im Kalkalpin Bayerns und Nordtirols (Inkohlung und Illit-Kristallinität). Ph. D. thesis, Frankfurter geowiss. Arbeiten, Serie C, Vol. 10, 259 p.

SCHERRER, P. (1918): Bestimmung der Grösse und der inneren Struktur von Kolloidteilchen mittels Röntgenstrahlen. Göttinger Nachr. Math. Phys. 2, 98–100.

WEAVER, C.E. (1960): Possible uses of clay minerals in search for oil. Bull. Amer. Assoc. Petrol. Geol. 44, 1505–1518.